AFRL-RZ-WP-TP-2012-0091

ASSESSMENT OF CHEMICAL SOLUTION SYNTHESIS AND PROPERTIES OF $Gd_2Zr_2O_7$ THIN FILMS AS BUFFER LAYERS FOR SECOND-GENERATION HIGH-TEMPERATURE SUPERCONDUCTOR WIRES (POSTPRINT)

T. Aytug

University of Tennessee

M. Paranthaman, K.J. Leonard, H.Y. Zhai, M.S. Bhuiyan, E.A. Payzant, A. Goyal, S. Sathyamurthy, D.B. Beach, P.M. Martin, and D.K. Christen

Oak Ridge National Laboratory

X. Li, T. Kodenkandath, U. Schoop, and M.W. Rupich

American Superconductor Corp.

H.E. Smith, T. Haugan, and P.N. Barnes

Mechanical Energy Conversion Branch
Energy/Power/Thermal Division

FEBRUARY 2012

AIR FORCE RESEARCH LABORATORY
PROPULSION DIRECTORATE
WRIGHT-PATTERSON AIR FORCE BASE, OH 45433-7251
AIR FORCE MATERIEL COMMAND
UNITED STATES AIR FORCE

REPORT DOCUMENTATION PAGE

Form Approved
OMB No. 0704-0188

1. REPORT DATE *(DD-MM-YY)*	2. REPORT TYPE	3. DATES COVERED *(From - To)*
February 2012	Journal Article Postprint	01 January 2003 – 01 January 2005

4. TITLE AND SUBTITLE

ASSESSMENT OF CHEMICAL SOLUTION SYNTHESIS AND PROPERTIES OF $Gd_2Zr_2O_7$ THIN FILMS AS BUFFER LAYERS FOR SECOND-GENERATION HIGH-TEMPERATURE SUPERCONDUCTOR WIRES (POSTPRINT)

5a. CONTRACT NUMBER
In-house

5b. GRANT NUMBER

5c. PROGRAM ELEMENT NUMBER
62203F

6. AUTHOR(S)

T. Aytug (University of Tennessee)
M. Paranthaman, K.J. Leonard, H.Y. Zhai, M.S. Bhuiyan, E.A. Payzant, A. Goyal, S. Sathyamurthy, D.B. Beach, P.M. Martin, and D.K. Christen (Oak Ridge National Lab)
X. Li, T. Kodenkandath, U. Schoop, & M.W. Rupich (American Superconductor Corp.)
H.E. Smith, T. Haugan, and P.N. Barnes (AFRL/RZPG)

5d. PROJECT NUMBER
3145

5e. TASK NUMBER
32

5f. WORK UNIT NUMBER
314532Z9

7. PERFORMING ORGANIZATION NAME(S) AND ADDRESS(ES)

University of Tennessee
Department of Physics and Astronomy
Knoxville, TN 37996

Oak Ridge National Laboratory
Oak Ridge, TN 37831

American Superconductor Corp.
Westborough, MA 01581

Mechanical Energy Conversion Branch (AFRL/RZPG)
Energy/Power/Thermal Division
Air Force Research Laboratory, Propulsion Directorate
Wright-Patterson Air Force Base, OH 45433-7251
Air Force Materiel Command, United States Air Force

8. PERFORMING ORGANIZATION REPORT NUMBER
AFRL-RZ-WP-TP-2012-0091

9. SPONSORING/MONITORING AGENCY NAME(S) AND ADDRESS(ES)

Air Force Research Laboratory
Propulsion Directorate
Wright-Patterson Air Force Base, OH 45433-7251
Air Force Materiel Command
United States Air Force

10. SPONSORING/MONITORING AGENCY ACRONYM(S)
AFRL/RZPG

11. SPONSORING/MONITORING AGENCY REPORT NUMBER(S)
AFRL-RZ-WP-TP-2012-0091

12. DISTRIBUTION/AVAILABILITY STATEMENT
Approved for public release; distribution unlimited.

13. SUPPLEMENTARY NOTES

Journal article published in *Journal of Materials Research*, Vol. 20, No. 11, November 2005. Work on this effort was completed in 2005.

PA Case Number: AFRL/WS-05-0920; Clearance Date: 06 Dec 2005.

14. ABSTRACT

Chemical solution processing of $Gd_2Zr_2O_7$ (GZO) thin films via sol-gel and metalorganic decomposition (MOD) precursor routes have been studied on textured Ni-based tape substrates. Even though films processed by both techniques showed similar property characteristics, the MOD-derived samples developed a high degree of texture alignment at significantly lower temperatures. Both precursor chemistries resulted in exceptionally dense, pore-free, and smooth microstructures, reflected in the cross-sectional and plan-view high-resolution scanning and transmission electron microscopy studies. On the MOD GZO buffered Ni–3at.% W (Ni–W) substrates with additional CeO_2/YSZ sputtered over layers, a 0.8-μm-thick $YBa_2Cu_3O_{7-\delta}$ (YBCO) film, grown by an ex situ metalorganic trifluoroacetate precursor method, yielded critical current, I_c (77 K, self-field), of 100 A/cm width. Furthermore, using pulsed-laser deposited YBCO films, a zero-field superconducting critical current density, J_c (77 K), of 1×10^6 A/cm^2 was demonstrated on an all-solution, simplified CeO_2(MOD)/GZO(MOD)/Ni–W architecture. The present study establishes GZO buffers as a candidate material for low-cost, all-solution coated conductor fabrication.

15. SUBJECT TERMS
solution, films, textured, sputtered, layers, temperatures, precursor, metalorganic, substrates, decomposition, electron, microscopy

16. SECURITY CLASSIFICATION OF:			17. LIMITATION OF ABSTRACT:	18. NUMBER OF PAGES	19a. NAME OF RESPONSIBLE PERSON (Monitor)
a. REPORT	b. ABSTRACT	c. THIS PAGE			Timothy J. Haugan
Unclassified	Unclassified	Unclassified	SAR	16	19b. TELEPHONE NUMBER *(Include Area Code)* N/A

Assessment of chemical solution synthesis and properties of $Gd_2Zr_2O_7$ thin films as buffer layers for second-generation high-temperature superconductor wires

T. Aytug[a)]
Oak Ridge National Laboratory, Oak Ridge, Tennessee 37831; and Department of Physics and Astronomy, University of Tennessee, Knoxville, Tennessee 37996

M. Paranthaman, K.J. Leonard, H.Y. Zhai, M.S. Bhuiyan, E.A. Payzant, A. Goyal,[b)] S. Sathyamurthy, D.B. Beach, P.M. Martin, and D.K. Christen
Oak Ridge National Laboratory, Oak Ridge, Tennessee 37831

X. Li, T. Kodenkandath, U. Schoop, and M.W. Rupich
American Superconductor Corp., Westborough, Massachusetts 01581

H.E. Smith, T. Haugan, and P.N. Barnes
Air Force Research Laboratory, Materials and Manufacturing Directorate, Wright-Patterson AFB, Ohio 45433

(Received 3 May 2005; accepted 21 July 2005)

Chemical solution processing of $Gd_2Zr_2O_7$ (GZO) thin films via sol-gel and metalorganic decomposition (MOD) precursor routes have been studied on textured Ni-based tape substrates. Even though films processed by both techniques showed similar property characteristics, the MOD-derived samples developed a high degree of texture alignment at significantly lower temperatures. Both precursor chemistries resulted in exceptionally dense, pore-free, and smooth microstructures, reflected in the cross-sectional and plan-view high-resolution scanning and transmission electron microscopy studies. On the MOD GZO buffered Ni–3at.% W (Ni–W) substrates with additional CeO_2/YSZ sputtered over layers, a 0.8-μm-thick $YBa_2Cu_3O_{7-\delta}$ (YBCO) film, grown by an ex situ metalorganic trifluoroacetate precursor method, yielded critical current, I_c (77 K, self-field), of 100 A/cm width. Furthermore, using pulsed-laser deposited YBCO films, a zero-field superconducting critical current density, J_c (77 K), of 1×10^6 A/cm^2 was demonstrated on an all-solution, simplified CeO_2(MOD)/GZO(MOD)/Ni–W architecture. The present study establishes GZO buffers as a candidate material for low-cost, all-solution coated conductor fabrication.

I. INTRODUCTION

The conduction of electric currents in the absence of resistivity at cryogenic temperatures (30–77 K) offers great potential for energy saving applications of high temperature superconductor (HTS) wires (HTS-coated conductors) in the electric utility and power sectors. In fact, HTS wires can carry 200 times the electrical current of equivalent conventional copper wires and has the potential to save up to 20% of electrical energy that is now lost to Joule heating in transmission and distribution. Second-generation, coated conductor HTS wire is a layered composite composed of (i) deposited high temperature superconductor compound, usually $YBa_2Cu_3O_{7-\delta}$ (YBCO), and (ii) intermediate oxide or metal buffer layers on (iii) a metal/metal-alloy substrate.[1] The coated conductor approach has achieved excellent wire performance, stemming from the fact that the percolative superconducting current flow occurs through a network of low-angle grain boundaries, leading to critical current density values (J_c), which are similar to those obtained on single crystal substrates.[3] While this performance level is a key for the commercial realization of HTS wires, decreasing cost of the conductor still remains a central issue for penetration in commercial markets. Hence, avoiding expensive vacuum processing in each fabrication step (i.e., HTS and buffer-layer) would potentially aid to meet the Department of Energy price/performance target level of $10/kA m.[4]

One of the leading, potentially economic approaches to fabricate HTS wires is the so-called rolling–assisted biaxially textured substrates (RABiTS).[1–3] Moreover,

[a)]Address all correspondence to this author.
e-mail: aytugt@ornl.gov
[b)]This author was an editor of this journal during the review and decision stage. For the *JMR* policy on review and publication of manuscripts authored by editors, please refer to http://www.mrs.org/publications/jmr/policy.html.
DOI: 10.1557/JMR.2005.0365

non-vacuum based chemical solution deposition processes such as sol-gel, chelate, and/or metalorganic decomposition (MOD) have proven to be a viable low-cost high-volume manufacturing technology for long-length practical wires.[5,6] Solution chemistry has the advantage of atomic-scale mixing of species, precise control of metal-oxide precursor stoichiometry, as well as near 100% utilization of the precursor material.

Presently, buffer layer architectures on which high-J_c YBCO films have been consistently obtained comprise the three layers CeO_2/yttrium-stabilized zirconia (YSZ)/(Y_2O_3 or CeO_2), deposited epitaxially on Ni-alloy substrates by physical vapor deposition (PVD) techniques.[4,7,8] Recently, there have been significant efforts concentrated on chemical solution derived $SrTiO_3$, RE_2O_3, $RE_2Zr_2O_7$, and RE_3NbO_7 (RE = rare-earth) films to assess their feasibility as buffer layer materials on RABiTS.[6,9–13] Among these systems, sol-gel processed single $La_2Zr_2O_7$ (LZO) buffer layers, a $RE_2Zr_2O_7$-based cubic pyrochlore structure, as well as LZO seeds capped with sputtered CeO_2/YSZ layers have shown the most promise as templates for YBCO with high-J_c performance.[10,14] Despite similar precursor processing chemistries, the other solution based material systems have not yet demonstrated performance levels as effective as $RE_2Zr_2O_7$. Currently, studies to understand the relationship between the processing techniques and the role of various materials are being pursued by many others.[9–14]

Another $RE_2Zr_2O_7$-based material that has recently been drawing considerable interest is $Gd_2Zr_2O_7$ (GZO), with a pseudocubic lattice parameter of 3.72 Å. To date, fabrication of GZO has been made by using ion-beam-assisted deposition (IBAD), a vacuum-based approach for biaxially textured template fabrication, where it was realized that a factor-of-two increase in the processing rate can be obtained over the original IBAD-YSZ process.[15,16] Subsequently, it was found that the CeO_2 films deposited on IBAD-GZO layers exhibit significantly improved grain alignment (i.e., small in-plane mosaic spread). Hence, it is of essence to assess the solution deposition technology for GZO films on the RABiTS template.

In this study, we investigated the viability of GZO as a buffer layer via wet chemical precursor approaches. In particular, growth and microstructural behavior of GZO layers were examined. Contrary to the common observation of porous microstructure in solution processed oxide layers, GZO films studied in this initial work were dense and free of pores. We have also demonstrated high-J_c YBCO performance on these GZO buffers with sputtered and MOD-derived CeO_2 cap layers.

II. EXPERIMENTAL

The RABiTS technique employs a well-established progressive rolling deformation process (95–98%) followed by recrystallization annealing step to obtain sharp biaxially cube-textured metal tapes, with ⟨100⟩ face-centered-cubic (fcc) crystalline axes aligned along both the rolling direction and perpendicular to the tape plane. These single-crystal-like, flexible metal substrates in tape or sheet form, are tens of centimeters in width and 50 μm in thickness. Both pure Ni (99.99%) and Ni–3 at.% W (Ni–W) substrates were used. Preparation of the substrates has been described in detail elsewhere.[3,17]

Both sol-gel and MOD routes were used to prepare precursor GZO solutions. Sol-gel solution preparation was carried out under an Ar gas atmosphere using a Schlenck-type apparatus and the MOD precursors were made in ambient atmosphere. To avoid premature hydrolysis, which can induce precipitation, the as-received gadolinium acetate (Alfa, purity: 99.9%, Ward Hill, MA) powder was first purified by dissolving in a mixture of water and acetic acid at a ratio of 3:1. The solution was filtered and then evaporated to dryness in an oven maintained at 150 °C for overnight to remove absorbed moisture. For the sol-gel chemistry, a stoichiometric mixture of purified gadolinium acetate and zirconium *n*-propoxide in 70% w/w *n*-proponal (Alfa) were dissolved and refluxed in excess of 2-methoxyethanol (Alfa, 99%) in a 250 ml round-bottomed flask. The acetic acid (Alfa, 99.99%) and 2-proponal formed during the exchange reaction was distilled out along with the excess 2-methoxyethanol. The final concentration of the solution was adjusted to 0.25 M of total cations. The MOD solution was prepared from the purified gadolinium acetate by first dissolving it in acetic acid and then mixing with stoichiometric amount of zirconium acac (Alfa) while continuously stirring at room temperature. The final volume is adjusted to 20 ml to produce a 0.25 M cation precursor solution. The coatings were done by spin-coating on 1 cm wide substrates at 4000 rpm for 30 s followed by direct heating to the crystallization temperature in a reducing atmosphere of forming gas (Ar + 4% H_2). To optimize the GZO growth conditions, samples were annealed at various temperatures ranging from 1050 to 1250 °C for 30 min.

The YBCO films were deposited by pulsed laser deposition (PLD) at 780 °C in 200 mTorr oxygen with an average energy density of ~2 J/cm^2/pulse. Following deposition, the films were annealed under 550 Torr oxygen during cool down. The samples were characterized for crystal structure, phase purity, and texture by using x-ray diffraction (XRD), with high temperature XRD to document the nucleation and growth. Scanning electron (SEM) and high-resolution transmission electron microscopy (HRTEM), equipped with energy dispersive spectrometry (EDS), were used for homogeneity, microstructure, and cross-sectional examinations. We used atomic force microscopy (AFM) for surface roughness analysis. Secondary ion mass spectroscopy (SIMS) depth-profile

analyses were conducted to study the chemical compatibility and diffusion of elemental products through the conductor stack, as related to the possible cation contamination of YBCO. For the SIMS, an oxygen primary ion beam was used. The major isotope of each element was followed, and spectrometer mass resolution was set at $M/\Delta M = 3000$ (10% valley) to exclude the contributions of other possible interferences. Electrical properties such as the resistive superconducting transition temperature (T_c), critical current density (J_c), and current-voltage (I-V) characteristics of the composite structures were evaluated by a standard four-probe technique. Values of J_c were assigned at a 1 μV/cm criterion.

III. RESULTS

While GZO buffer layers processed by both sol-gel and MOD routes were stable up to a maximum processing temperature (T) of 1250 °C, sol-gel synthesized GZO films required temperatures above 1200 °C to obtain good crystalline quality. Figure 1 shows the XRD out-of-plane ($\Delta\omega$) and in-plane ($\Delta\phi$) full width at half-maximum (FWHM) peak-width distributions for GZO (004) and (222) reflections as a function of processing temperature. For direct quantitative comparison between the crystalline quality of the samples, FWHM values are normalized to those of the underlying Ni substrate. While the processing temperature does not have substantial effect on the in-plane alignment of the GZO films, the degree of mosaic spread of the GZO layers sharpens up significantly with increasing temperature above 1100 °C and continues to gradually improve up to temperatures around 1200 °C. These results are expected because, during the transformation of amorphous to crystalline phase, heterogeneous nucleation events occur preferentially at the substrate interface due to the lower interfacial energy.

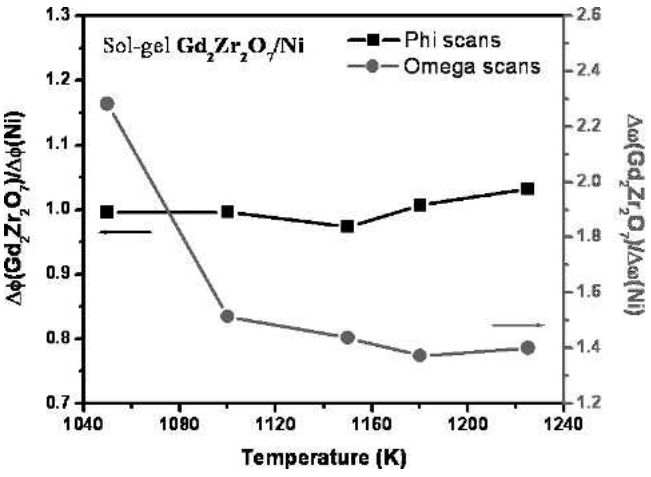

FIG. 1. Dependence of the normalized XRD FWHM peak widths on processing temperatures, quantifying the crystallinity of sol-gel $Gd_2Zr_2O_3$ films: (i) out-of-plane distribution width $\Delta\omega$ and (ii) in-plane distribution width $\Delta\phi$.

As such, the in-plane alignment of GZO films is primarily governed by the crystallographic texture of and epitaxy with the underlying substrate. On the other hand, the observed improvement in out-of-plane texture of GZO is a direct consequence of the processing temperature, where the thermal energy assists to align misoriented grains, reducing the mosaic spread. In fact, improvement of texture alignment can be clearly observed in the logarithmic scale (222) pole figures for GZO films that were processed between 1050 and 1225 °C for 1 h in flowing Ar+4%H_2 [Figs. 2(a)–2(d)]. For processing temperatures <1200 °C, significant amount of misoriented grains are present along with less well defined poles; and the quantitative analysis of the pole figure intensities indicates that the samples are < 90% cube textured (Fig. 3). On the other hand, a well-developed, 95% single-component cube texture is evident for the sample annealed at 1225 °C. It is well known that non-textured materials can result in undesirable high-angle grain boundaries, which are proven to severely limit the super current flow in the HTS film. Despite the development of good texture, the out-of-plane alignment of GZO films did not sharpen to the level of the substrate even upon annealing at 1225 °C. This may be a consequence of chemical and physical properties of the substrate surface, thermal processing conditions and/or the precursor chemistry of the sol-gel process. Besides, such high temperatures could also induce secondary recrystallization in technologically viable Ni-based alloy substrates, resulting in significant fraction of random texture formation. Hence, these results challenged us to develop more practical solution routes to fabricate GZO layers on Ni-based substrates. Hereafter, the processing conditions and physical properties of GZO layers synthesized only by the MOD solution method will be discussed.

First, nucleation and growth behavior of MOD GZO layers were determined by in situ XRD studies. Experiments were carried out in a Scintag PAD X diffractometer with a linear position sensitive detector covering a 2θ range of 8° centered at $2\theta = 31°$ in reducing Ar + 2%He atmosphere. A single-coat GZO film, approximately 15–20 nm thick, on a Ni–W substrate was heated from room temperature to 1250 °C on a rhodium-platinum strip heater at a heating rate of 400 °C/min. XRD patterns were recorded for a series of temperatures (data not shown here). Film crystallization nucleated at about 700 °C and phase formation was completed around 1100–1150 °C, which was evidenced by the saturation of the GZO (004) peak intensity with further increase in temperature up to 1250 °C. We have not observed any indication of polycrystalline GZO component formation at the temperature range studied. This result reflects a significantly lower (75–125 °C) processing temperature to form epitaxial structure through MOD precursor chemistry. Even though there is no direct evidence, the

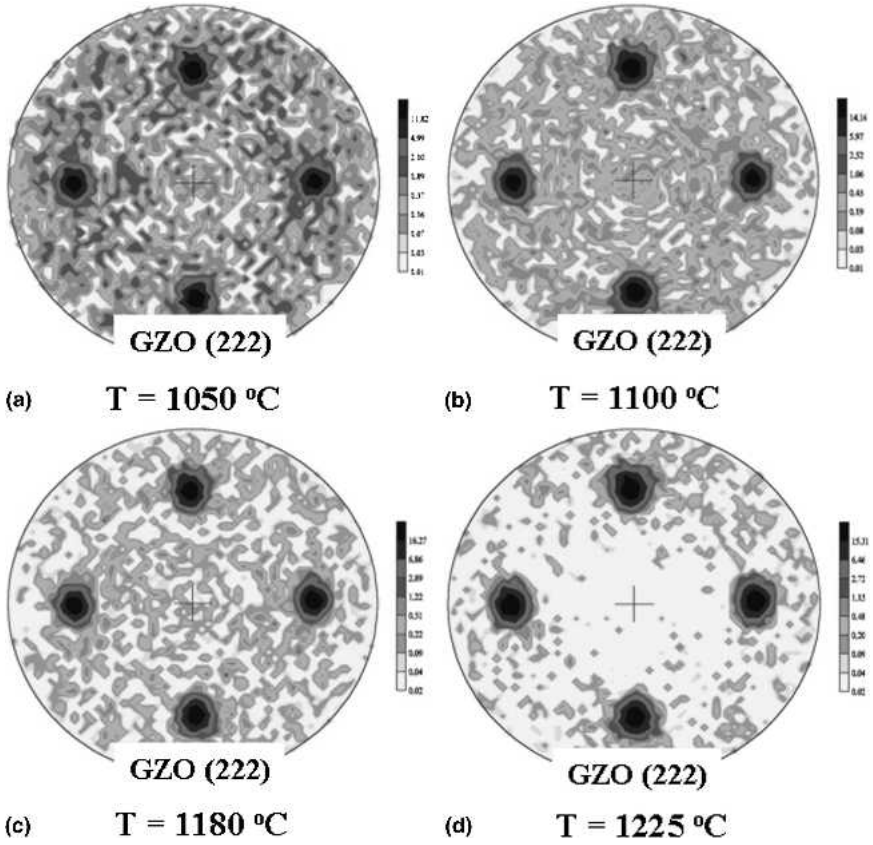

FIG. 2. XRD pole figures for $Gd_2Zr_2O_7$ layers on pure Ni substrates, plotted on a logarithmic scale, for processing at various temperatures. (a) 1050 °C, (b) 1100 °C, (c) 1180 °C, and (d) 1225 °C.

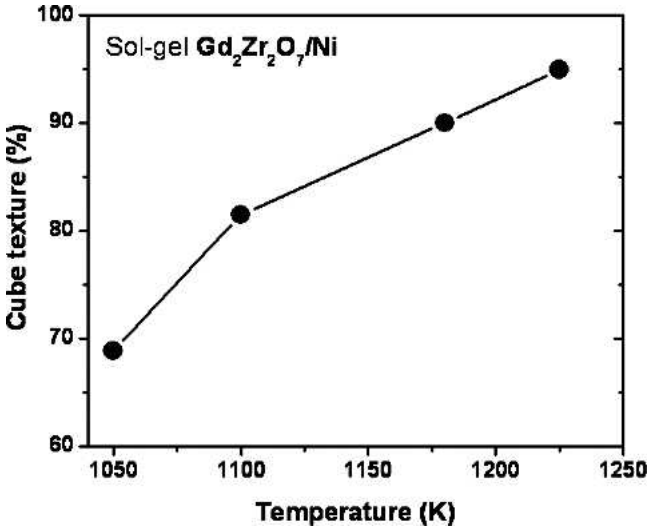

FIG. 3. Pole figure cube-texture percentages as determined by the quantitative analysis of the pole intensities for the samples shown in Fig. 2.

reason for the observed decrease in processing temperature could be due to the differences in precursor chemistries of sol-gel and MOD-derived films. Moreover, high-temperature XRD studies also revealed that the film growth is completed within 5 min when heat treated at 1150 °C. For this study, another single-coat GZO sample was heated to 1150 °C at the same heating rate, with XRD patterns collected every 30 s for 60 min. In general, decrease in processing temperature should ease the fabrication requirements and provide a more practical synthesis scheme on Ni–W as well as on other technologically viable substrates.

After having established the basic relationship between the phase nucleation and growth characteristics via MOD approach, GZO films with thicker coatings were produced by multiple spin coatings with intermediate annealing steps. Thicker coatings are generally required due to the substrate cation diffusion issues associated with bulk porosity in solution processed buffer layers. Figure 4 shows the XRD θ-2θ spectrum of 1–3-layer coatings processed at 1150 °C. Each coat is typically 15–20 nm thick. Clearly, the GZO (004) peak intensity increases with each successive coat as the intensity of polycrystalline GZO (111) component remains at the background levels.

In Fig. 5(a), a typical plan-view high-resolution SEM microstructure of a single-coat GZO film is presented in the vicinity of a grain boundary. The sample exhibits a dense, continuous, and crack-free morphology with

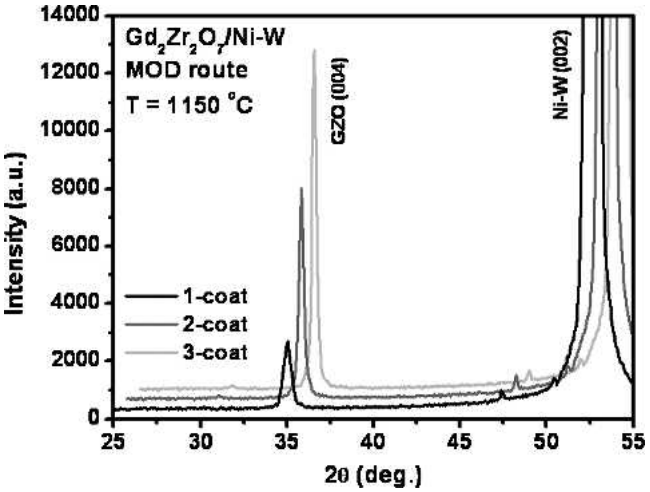

FIG. 4. XRD θ-2θ spectra of 1-3 coats of $Gd_2Zr_2O_7$ layers on textured Ni–W substrates, showing a monotonic increase in the (004) intensity with the number of coats.

uniform coverage at the grain boundary. AFM measurements [Fig. 5(b)] show that the GZO film has a narrow distribution of nanoscale growth nuclei. The root-mean-square roughness (R_a) on a 10 × 10 μm area is 3 nm, which is comparable to that of the underlying substrate (R_a = 1 nm). A more detailed roughness profile, obtained without averaging, can be seen from the line scan analysis on a 5 × 5 μm region [Fig. 5(c)]. No significant variations in the surface profile along the line scan are observed, indicative of spatially uniform film growth. Cross-section examination of GZO films on Ni–W substrates revealed a number of interesting growth characteristics. For comparison, TEM images of the thinned cross-sectional area of a single coat sol-gel and a three coat MOD derived GZO films are shown together in Figs. 6(a) and 6(b). While both samples show a dense microstructure and complete *c*-axis-oriented growth throughout the thickness, the sol-gel GZO sample exhibit a rougher surface. This is likely due to the processing at a relatively higher temperature than MOD films (T = 1250 versus 1150 °C). For this particular sol-gel sample, the GZO thickness varies between 13–23 nm, with an average thickness of 19 nm. Epitaxial orientation of the GZO and Ni–W substrate can be seen within the selected area electron diffraction pattern [Figs. 6(c)], showing that the GZO layer was oriented with its ⟨001⟩ direction normal to the interface, and producing a rotated cube-on-cube orientation of GZO⟨110⟩//Ni–W⟨100⟩. A closer look at the interface of both samples [Fig.7(a) for sol-gel and 7(b) for MOD sample] revealed no evidence of reactions between the GZO film and substrate or presence of any secondary phases within the GZO layers. In fact, an EDS line scan across the boundary between the sol-gel derived film and Ni–W substrate [Fig. 7(c)], using an electron probe of approximately 1.5 nm diameter, displays sharp changes in the Gd, Zr, and Ni signals at the interface, providing further support for a clean interface and no significant intermixing. Most interestingly, unlike the common observations reported in solution processed films (i.e., sol-gel $La_2Zr_2O_7$ or MOD YBCO),

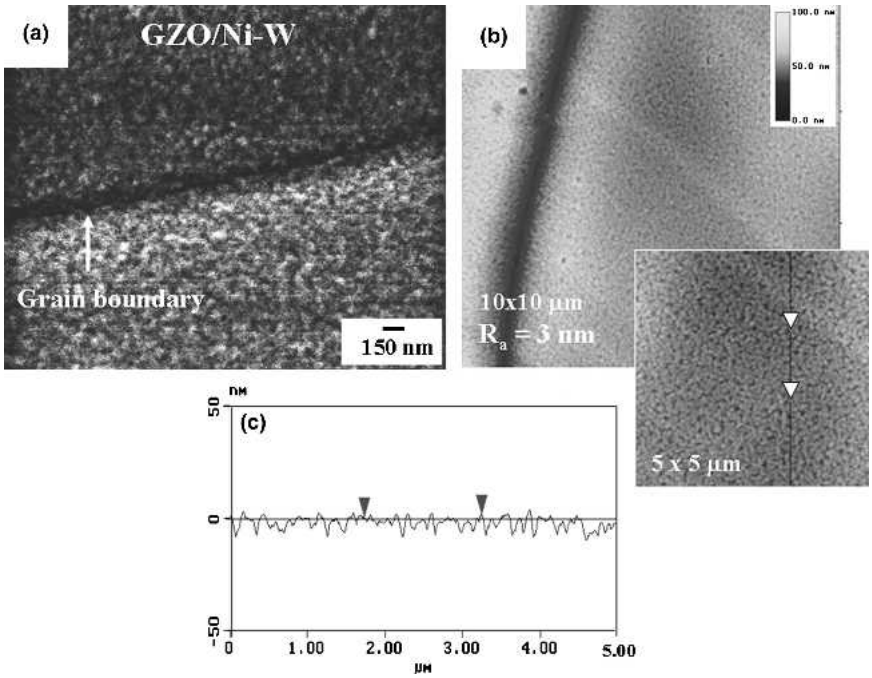

FIG. 5. Surface microstructure of a single coat $Gd_2Zr_2O_7$ film investigated by (a) high-resolution SEM, (b) AFM, and (c) AFM surface profile on a 5 μm line scan (small image).

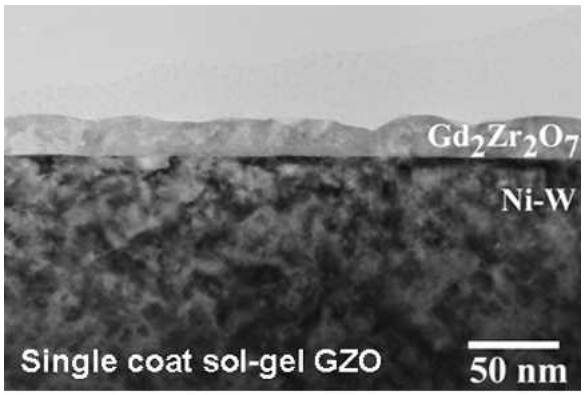

(a)

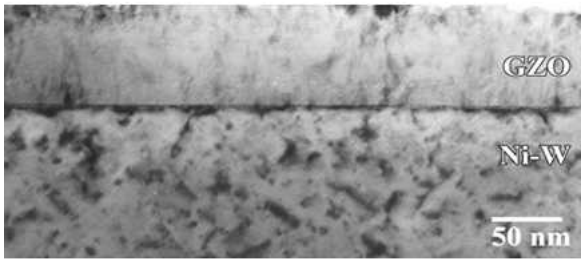

(b)

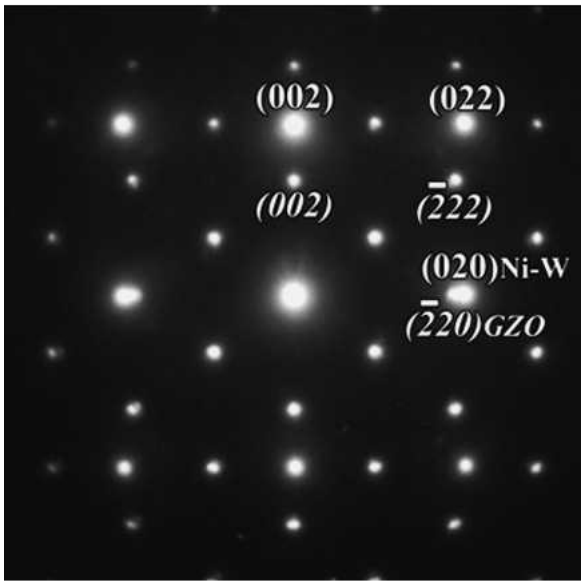

(c)

FIG. 6. Cross-section TEM images of the (a) single-coat sol-gel and (b) three-coat MOD processed $Gd_2Zr_2O_7$ films on Ni–W substrates. (c) Selected area diffraction pattern illustrating the Ni–W⟨100⟩// $Gd_2Zr_2O_7$⟨110⟩ rotated cube-on-cube epitaxial relationship between the films and substrates.

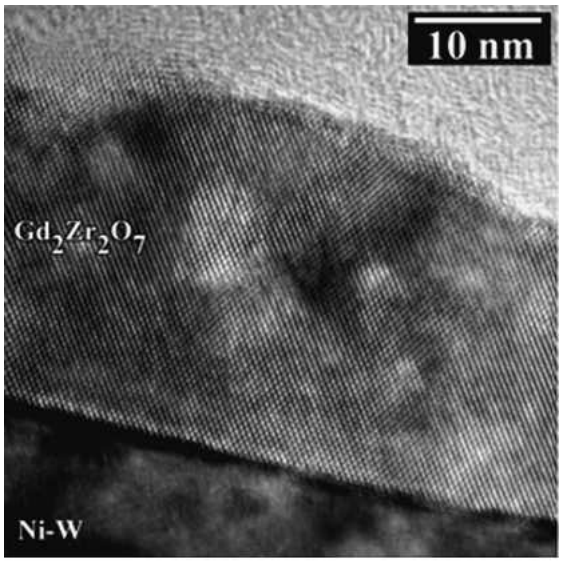

(a)

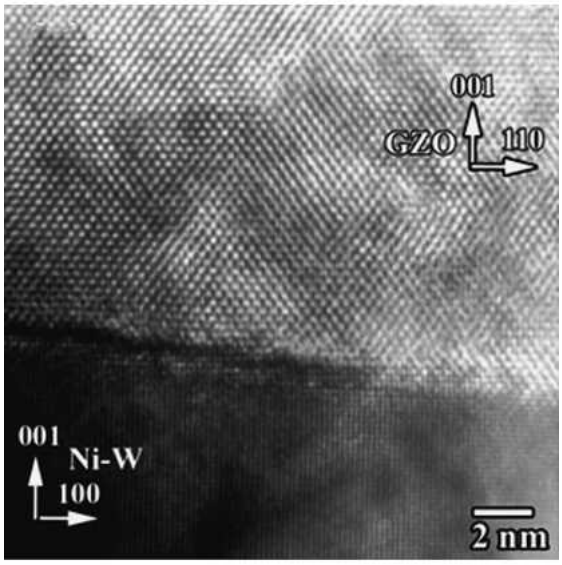

(b)

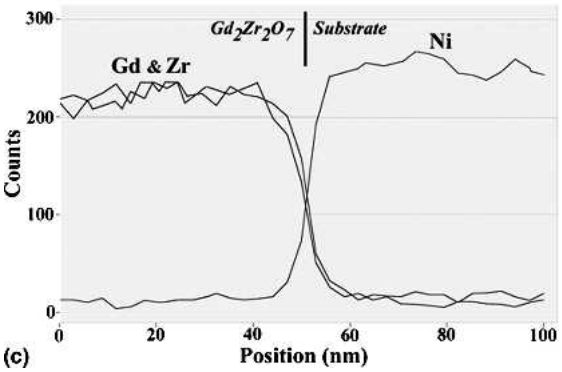

(c)

FIG. 7. High-resolution TEM images of the interface between $Gd_2Zr_2O_7$ and Ni–W for (a) the single coat sol-gel and (b) the three-coat MOD deposited film revealing a pore-free and dense microstructure. (c) EDS nano-probe line scan across the GZO/Ni–W interface, verifying a clean and sharp interface with no interfacial reactions or interdiffusion.

these high-resolution TEM images show no porosity in GZO layers prepared by either technique. Although further work is required to understand the underlying mechanisms for this favorable growth behavior, it may in part be related to the chemical nature of the precursor species, such that the onset of crystallization is delayed to

higher temperatures, therefore enhancing the film densification. This is a significant observation, since pores along with other structural defects can act as accelerated pathways for inward diffusion of oxygen to the metal substrate as well as outward diffusion of substrate cations to the HTS layer, degrading the physical properties of the conductor. Obviously, eliminating such defects from any buffer architecture should improve the performance of a coated conductor structure. The SIMS data shown in Fig. 8 are consistent with these observations of good growth behavior. The interfaces between layers in the sputter depth profile are sharp and do not show the sputter profile broadening and degradation with increasing depth that is typically observed with porous or rough films. The linear, normalized signal representation used here is chosen as the appropriate representation to reveal any possible cation diffusion. The apparent diffusion of small amounts of copper from the YBCO layer into the GZO layer may be SIMS beam-induced Cu segregation known to occur in the profiling of oxides.[18] Small amounts of Ce signal seem to have diffused into the topmost portion of the GZO layer. In that portion of the film, Zr has greater signal than in the remainder. Gd and C signals are correspondingly low in this portion of the GZO layer, rising to full value in the deeper portion of the layer. In the light of the transmission electron microscopy HRTEM-EDS scan of Fig. 7, this may be a SIMS ion enhancement effect due to differing chemical environment through the GZO layer, specifically caused by the variable carbon distribution.

The performance of the MOD GZO buffer layers was evaluated by depositing both in situ PLD and ex situ metalorganic trifluoroacetate (TFA)-based YBCO coatings. The latter was used in our initial test. First, CeO_2/YSZ buffer layers were deposited by magnetron sputtering on a single layer GZO coated Ni/Ni–W substrate. A CeO_2 cap layer was used to provide an optimized structural and chemical template for TFA YBCO growth. The intermediate YSZ layer serves as a barrier for Ni diffusion. Chemical compatibility is especially crucial for ex situ grown YBCO films. Details of the TFA process are presented in Ref. 19. Figure 9 illustrates the current-voltage characteristics of a 0.8-μm-thick TFA-based YBCO film on such a substrate. The sample exhibited a self-field critical current (I_c) of 100 A/cm width, which corresponds to $J_c = 1.25 \times 10^6$ A/cm^2. Although this result does not reflect optimum performance, it demonstrates that MOD-synthesized GZO films can act as good templates for further growth of epitaxial oxide layers. Next, in an attempt to simplify the entire structure, we removed the YSZ layer from the buffer architecture for in situ deposition of YBCO. In Fig. 10, we compare the magnetic field (H) dependence of transport J_c at 77 K for two PLD YBCO films. These films were deposited on three coat GZO buffers (~60 nm thick), capped with both sputtered and solution (MOD) derived CeO_2 layers (~20 nm thick). Measurements are made with the field applied parallel to the c-axis. Details of CeO_2 fabrication by either solution or sputtering techniques have been reported elsewhere.[4,7,20] The zero-field J_c value for a 0.2-μm-thick YBCO film on an all-solution processed CeO_2(solution)/GZO(solution)/Ni–W is 1×10^6 A/cm^2, and the superconducting transition temperature T_c is around 92 K (see inset). A J_c (self-field) of 1.1×10^6 A/cm^2 is obtained for a thicker YBCO film (0.5 μm) on CeO_2(sputtered)/GZO(solution)/Ni–W, which reflects performance comparable to that on standard vacuum-based three-layer CeO_2/YSZ/Y_2O_3 buffer architecture. Since the YBCO is thicker in the latter case and an exponential decrease in J_c with thickness for in situ YBCO coatings is well known,[21,22] the J_c–H data suggest that further optimization is required for MOD CeO_2 cap layers. In fact, the surface of some samples showed small amounts of polycrystalline CeO_2.

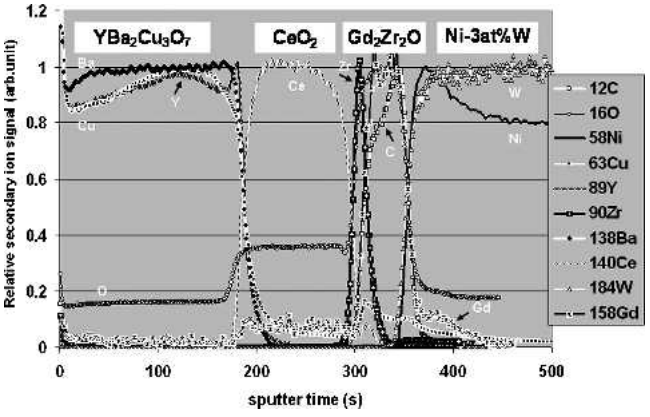

FIG. 8. SIMS depth profile of the three-coat MOD-processed GZO/Ni–W sample, showing major element distributions throughout the sample. The intensity scale for each element is normalized to its maximum value. Sputter time is proportional to depth, but sputter rates of layers differ.

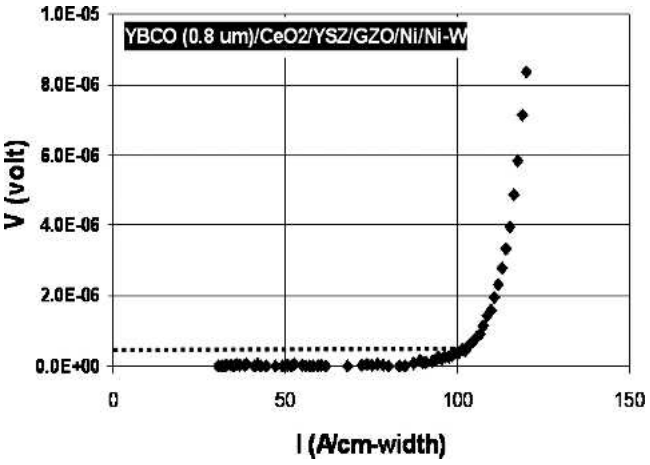

FIG. 9. Current–voltage curve of a YBCO/CeO_2/YSZ/GZO/Ni/Ni–W sample, where YBCO is processed via the ex situ TFA approach. The dashed line indicates the voltage criterion for definition of I_c.

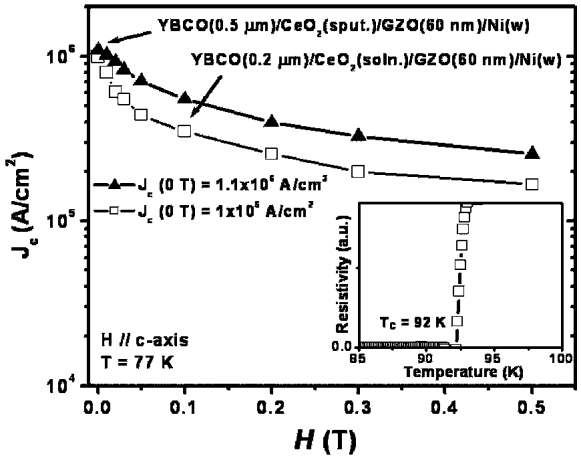

FIG. 10. Magnetic field dependence of J_c measured at 77 K for two YBCO films deposited by PLD on the (i) all-solution MOD CeO_2 and (ii) sputtered CeO_2 capped $Gd_2Zr_2O_7$(MOD)/Ni–W. The inset shows the resistive superconducting transition region for the former sample.

Such random crystallites are possibly a result of surface nucleation associated with competition between the crystallization driving forces, where the free surface nucleation becomes as plausible as interface nucleation at the growth conditions used for MOD CeO_2 films. Cross-sectional TEM investigations (not shown) depicted no indication of homogeneous random nucleation. An additional issue is that the out-of-plane texture of MOD GZO films needs further improvement, evidenced by the slight increase in FWHM values of the ω scans on progressing from substrate to YBCO layer. For instance, while the in-plane alignment of individual layers in YBCO/CeO_2(sputtered)/GZO(solution)/Ni–W structure replicate the texture of the Ni–W substrate ($\Delta\phi = 8°$), the ω rocking curve FWHM are progressively broader, with value of 6.2°, 7.4°, 8.5°, and 8.6° for the Ni–W, GZO, CeO_2, and YBCO layers, respectively. This broadening in Δω may have been a contributing factor for the non-optimal transport J_c. Interestingly, a similar increase was also found in the out-of-plane texture of solution-based LZO and RE_2O_3 buffer systems, but no explanation was given for the cause.[10,11,23,24] Nevertheless, the present preliminary results indicate strong viability of solution-based GZO buffer layers for practical HTS-wire fabrication.

IV. SUMMARY

We have demonstrated that GZO films can be grown epitaxially on Ni–W substrates by sol-gel and MOD-based solution deposition processes. The effects of processing parameters on the growth of these buffers were studied. Remarkably, GZO films synthesized by both techniques showed dense and pore-free microstructure, which were reflected within the examined cross-section microstructures. Studies also indicated that GZO films via MOD route can be processed at temperatures 75–125 °C lower than the sol-gel counterparts, easing the materials requirements on the technologically viable metal substrates. Through both the PLD and TFA methods, high-quality YBCO films have been obtained on MOD derived GZO films. On a CeO_2/YSZ/GZO/Ni–W architecture, 0.8-μm-thick TFA YBCO film exhibited I_c (77 K) values of 100 A/cm width. On a simplified, all-solution buffer architecture of CeO_2(solution)/GZO(solution)/Ni–W, we achieved self-field J_c (77 K) of 1.0×10^6 A/cm^2 for PLD-deposited 0.2-μm-thick YBCO films. These observations reflect the strong candidacy of MOD GZO buffers for low-cost, scalable second-generation HTS-wire manufacturing.

ACKNOWLEDGMENTS

This work was supported by the United States Department of Energy (USDOE), Office of Basic Energy Sciences and the Office of Electrical Transmission and Distribution. The research was performed at the Oak Ridge National Laboratory, managed by U.T.-Battelle, LLC for the USDOE under Contract No. DE-AC05-00OR22725.

REFERENCES

1. D.P. Norton, A. Goyal, J.D. Budai, D.K. Christen, D.M. Kroeger, E.D. Specht, Q. He, B. Saffian, M. Paranthaman, C.E. Klabunde, D.F. Lee, B.C. Sales, and F.A. List: Epitaxial $YBa_2Cu_3O_7$ on biaxially textured nickel (001): An approach to superconducting tapes with high critical current density. *Science* **274,** 755 (1996).
2. A. Goyal, D.P. Norton, J.D. Budai, M. Paranthaman, E.D. Specht, D.M. Kroeger, D.K. Christen, Q. He, B. Saffian, F.A. List, D.F. Lee, P.M. Martin, C.E. Klabunde, E. Hatfield, and V.K. Sikka: High critical current density superconducting tapes by epitaxial deposition of $YBa_2Cu_3O_x$ thick films on biaxially textured metals. *Appl. Phys. Lett.* **69,** 1795 (1996).
3. A. Goyal, D.P. Norton, D.M. Kroeger, D.K. Christen, M. Paranthaman, E.D. Specht, J.D. Budai, Q. He, B. Saffian, F.A. List, D.F. Lee, E. Hatfield, P.M. Martin, C.E. Klabunde, J. Mathis, and C. Park: Conductors with controlled grain boundaries: An approach to the next generation, high-temperature superconducting wire. *J. Mater. Res.* **12,** 2924 (1997).
4. A.P. Malozemoff: http://www.amsuper.com/html/products/library/2g_white_paper_-_march_2004.pdf
5. M.W. Rupich, Q. Li, S. Annavarapu, C. Thieme, W. Zhang, V. Prunier, M. Paranthaman, A. Goyal, D.F. Lee, E.D. Specht, and F.A. List: Low cost Y–Ba–Cu–O coated conductors. *IEEE Trans. Appl. Supercond.* **11,** 2927 (2001).
6. M. Paranthaman, T.G. Chirayil, F. List, X. Cui, A. Goyal, D.F. Lee, E.D. Specht, P.M. Martin, R.K. Williams, D.M. Kroeger, J.S. Morrell, D.B. Beach, R. Feenstra, and D.K. Christen: Fabrication of long lengths of epitaxial buffer layers on biaxially textured nickel substrates using a continuous reel-to-reel dip-coating unit. *J. Am. Ceram. Soc.* **84,** 273 (2001).
7. M. Paranthaman, D.F. Lee, A. Goyal, E. Specht, P.M. Martin, X. Cui, J.E. Mathis, R. Feenstra, D.K. Christen, and D.M. Kroeger: Growth of biaxially textured RE_2O_3 buffer layers

on rolled-Ni substrates using reactive evaporation for HTS-coated conductors. *Supercond. Sci. Technol.* **12,** 319 (1999).

8. F.A. List, A. Goyal, M. Paranthaman, D.P. Norton, E.D. Specht, D.F. Lee, and D.M. Kroeger: High J_c YBCO films on biaxially textured Ni with oxide buffer layers deposited using electron beam evaporation and sputtering. *Physica C* **302,** 87 (1998).
9. J.T. Dawley, R.J. Ong, and P.G. Clem: Chemical solution deposition of ⟨100⟩-oriented $SrTiO_3$ buffer layers on Ni substrates. *J. Mater. Res.* **17,** 1678 (2002).
10. S. Sathyamurthy, M. Paranthaman, H.Y. Zhai, S. Kang, T. Aytug, C. Cantoni, K.J. Leonard, E.A. Payzant, H.M. Christen, A. Goyal, X. Li, U. Schoop, A. Kodenkandath, and M.W. Rupich: Chemical solution deposition of lanthanum zirconate barrier layers applied to low-cost coated-conductor fabrication. *J. Mater. Res.* **19,** 2117 (2004).
11. T. Aytug, M. Paranthaman, S. Sathyamurthy, B.W. Kang, D.F. Lee, R. Feenstra, A. Goyal, P.M. Martin, and D.K. Christen: Reel-to-reel continuous chemical solution deposition of epitaxial Gd_2O_3 buffer layers on biaxially textured metal tapes for the fabrication of $YBa_2Cu_3O_{7-\delta}$ coated conductors. *J. Am. Ceram. Soc.* **86,** 257 (2003).
12. M. Paranthaman, M.S. Bhuiyan, S. Sathyamurthy, H.Y. Zhai, A. Goyal, and K. Salama: Epitaxial growth of solution-based rare-earth niobate, RE_3NbO_7, films on biaxially textured Ni–W substrates. *J. Mater. Res.* **20,** 6 (2005).
13. E. Celik, H. Okuyucu, I.H. Mutlu, M. Tomsic, J. Schwartz, and Y.S. Hascicek: Textured $La_2Zr_2O_7$, Gd_2O_3, and Er_2O_3 buffer layers for a long-length YBCO coated conductors by non-vacuum process. *IEEE Trans. Appl. Supercond.* **11,** 3162 (2001).
14. S. Sathyamurthy, B.W. Kang, T. Aytug, M. Paranthaman, P.M. Martin, A. Goyal, D.M. Kroeger, and D.K. Christen: Chemical solution deposition of lanthanum zirconate buffer layers on biaxially textured Ni–1.7% Fe–3% W alloy substrates for coated-conductor fabrication. *J. Mater. Res.* **17,** 1543 (2002).
15. Y. Iijima, K. Kakimoto, Y. Sutoh, S. Ajimura, and T. Saitoh: Development of long Y-123 coated conductors by ion-beam-assisted-deposition and the pulsed-laser-deposition method. *Supercond. Sci. Technol.* **17,** S264 (2004).
16. T. Kato, Y. Iijima, T. Muroga, T. Saitoh, T. Hirayama, I. Hirabayashi, Y. Yamada, T. Izumi, Y. Shiohara, and Y. Ikuhara: TEM observations of $Gd_2Zr_2O_7$ films formed by the ion-beam-assisted deposition method on an Ni-based alloy. *Physica C* **392–396,** 790 (2003).
17. A. Goyal, R. Feenstra, M. Paranthaman, J.R. Thompson, B.W. Kang, C. Cantoni, D.F. Lee, F.A. List, P.M. Martin, E. Lara-Curzio, C. Stevens, D.M. Kroeger, M. Kowalewski, E.D. Specht, T. Aytug, S. Sathyamurthy, R.K. Williams, and R.E. Ericson: Strengthened, biaxially textured Ni substrate with small alloying additions for coated conductor applications. *Physica C* **382,** 251 (2002).
18. C.J. Vriezema and P.C. Zalm: Impurity migration during SIMS depth profiling. *Surf. Interf. Anal.* **17,** 875 (1991).
19. M.W. Rupich, D.T. Verebelyi, W. Zhang, T. Kodenkandath, and X. Li: Metalorganic deposition of YBCO films for second-generation high-temperature superconductor wires. *MRS Bull.* **29**(8), 572 (2004).
20. M.S. Bhuiyan, M. Paranthaman, S. Sathyamurthy, T. Aytug, S. Kang, D.F. Lee, A. Goyal, E.A. Payzant, and K. Salama: MOD approach for the growth of epitaxial CeO_2 buffer layers on biaxially textured Ni–W substrates for YBCO coated conductors. *Supercond. Sci. Technol.* **16,** 1305 (2003).
21. S.R. Foltyn, P. Tiwari, R.C. Dye, M.Q. Le, and X.D. Wu: Pulsed-laser deposition of thick $YBa_2Cu_3O_{7-\delta}$ films with J_c-greater-than 1 MA/cm^2. *Appl. Phys. Lett.* **63,** 1848 (1993).
22. S.R. Foltyn, Q.X. Jia, P.N. Arendt, L. Kinder, Y. Fan, and J.F. Smith: Relationship between film thickness and the critical current of $YBa_2Cu_3O_{7-\delta}$-coated conductors. *Appl. Phys. Lett.* **75,** 3692 (1999).
23. T.G. Chirayil, M. Paranthaman, D.B. Beach, D.F. Lee, A. Goyal, R.K. Williams, X. Cui, D.M. Kroeger, R. Feenstra, D.T. Verebelyi, and D.K. Christen: Epitaxial growth of $La_2Zr_2O_7$ thin films on rolled Ni-substrates by sol-gel process for high T-c superconducting tapes. *Physica C* **336,** 63 (2000).
24. M. Paranthaman, T.G. Chirayil, S. Sathyamurthy, D.B. Beach, A. Goyal, F.A. List, D.F. Lee, X. Cui, S.W. Lu, B. Kang, E.D. Specht, P.M. Martin, D.M. Kroeger, R. Feenstra, C. Cantoni, and D.K. Christen: Fabrication of long lengths of YBCO coated conductors using a continuous reel-to-reel dip-coating unit. *IEEE Trans. Appl. Supercond.* **11,** 3146 (2001).